Available at www.sciencedirect.com

ScienceDirect

http://www.elsevier.com/locate/biombioe

Numerical modelling of a fixed bed updraft long stick wood gasifier

A. Saravanakumar [a,*], Mathew J. Hagge [b], T.M. Haridasan [a], Kenneth M. Bryden [b]

[a] NSP Green Energy Technologies Private Limited, Renewable Energy Research and Development, Flat No. 3, Mahaguru Apartment, Elim Nagar, 1st Main Road, Perungudi, Chennai 600 096, Tamil Nadu, India

[b] Department of Mechanical Engineering, Iowa State University, Ames, IA 50011-2161, USA

ARTICLE INFO

Article history:
Received 11 June 2008
Received in revised form
10 July 2011
Accepted 12 July 2011
Available online 6 August 2011

Keywords:
Numerical modelling
Casuarina equisetifolia species
Updraft gasifier
Transient state
Long stick wood

ABSTRACT

A computational model to evaluate the anticipated performance characteristics of an updraft fixed bed gasifier utilizing long stick wood as the source of fuel is presented. This type of gasifier obtains high-energy release rates due to the lower inlet air velocity and extended reaction zone. The numerical model couples the performance of the individual particles and the external gas phase reactions to describe the gasifier performance. By calculating the performance of individual particles, the computational model is able to determine the interaction between the combustion of charcoal particles in the lower portion of the bed and the pyrolysis of wood sticks in the upper region. Most importantly, the model can describe the effect on overall system performance when conditions within the gasifier are changed, such as changes in the wood or char particle size, moisture content, gasifier height, inlet velocity, etc. The results of the model are compared with the gasifier performance for a gasifier using sticks with a 6 cm diameter, a length of 68 cm and a dry density of 600 kg m^{-3}. The model results are used to investigate the performance of the gasifier under a variety of load conditions, fuel sizes, and moisture conditions.

1. Introduction

In this updraft gasifier, 60 kg of casuarina equisetifolia long stick wood sections are dried and pryolzed from the combustion of 10 kg of char. The wood is 6 cm in diameter × 68 cm in length and is stacked 60 cm high. The moisture content as received was 150 g kg^{-1} of total weight. The char is located below the wood and is 4.8 cm in diameter × 9 cm in length and stacked 48 cm high. For the first 10 min of operation, a fan operates in downdraft mode and fire ports are used during this ignition period to heat the char region to around 500 °C. Once stable ignition occurs, the fan is switched to an updraft mode, and the heat from the char combustion reactions is used to dry and gasify the packed bed of wood. The gasifier system runs for a period of 5 h and 15 min in the updraft configuration.

The wood particles are large enough that drying and pyrolysis occur within distinct regions of each wood particle. A char layer is rapidly formed on the outside of the sticks while wet wood remains within the stick. Pyrolysis products and moisture flow outward through the char layer cooling the surface and screening the surface from heat and mass transfer. Numerical modelling of this gasifier provides some significant challenges. The gasifier does not operate under steady-state conditions, and the overall bed cannot be separated into two distinct regions of drying and pyrolysis. The

* *Corresponding author*. Tel.: +91 9176686944.
E-mail address: sara_mnes@yahoo.co.in (A. Saravanakumar).
0961-9534/$ – see front matter © 2011 Elsevier Ltd. All rights reserved.
doi:10.1016/j.biombioe.2011.07.012

overall bed heat release rate is dependent on the heat and mass transfer to the long sticks; the formation of char layer; the reaction rate of the char with oxygen, carbon dioxide and water vapour; and the reaction rate of the pyrolysis products.

Both experimental and theoretical work provides a basis for the existence of two differing modes of wood combustion, defined as thermally thin and thermally thick [1,2]. In the case of small particles such as saw dust or rice husk, combustion occurs under thermally thin combustion; the time scale of heat transfer within the particles is much shorter than the time scale of convective heat transfer to the particle. Drying, pyrolysis and char combustion occur sequentially. In combustion of thermally thick fuel, the larger fuel wood size results in a thermal wave that drives the drying and pyrolysis of the particle. The fuel consists of a relatively unchanged core surrounded by a char layer.

Modelling of wood gasification is a dynamic area of research with many different areas being energetically pursued. Pyrolysis of thermally thin and thermally thick material and cellulose pyrolysis kinetics [3] provide an in depth review of cellulose pyrolysis kinetics. Limited data for large particles exist in coal combustion and gasification [4] and the state of the art for coal conversion has been well reviewed [13]. Wild fire specialists have studied ignition and mass loss for large wood particles as function of time for cylindrical wood elements with and without bark 2.5–10 cm in diameter [5]. The fixed bed combustion of large wood chips ($2 \times 2 \times 0.5$ cm) has been modelled [6] in a deep (20–40 cm) pressurized downdraft combustor gasifier. A larger scale 20 cm diameter hardwood log system has been analyzed in 3.7 m deep fuel bed [12] under similar conditions. Larger particles in gasification have been modelled for 2.5 cm diameter by 4 cm length with bed depth, particle size and moisture content as parameters [9], as well the modelling of 8 mm equivalent diameter char gasification [11]. Similar work with jute sticks (1 cm diameter, and 15 cm length) tied into 7.4 cm diameter aligned with the gas flow was modelled with a very thin 10 cm oxidation/reduction zone relative to the reaction chamber length of 1.5 m [10]. Saravanakumar and colleagues have tested an updraft gasifier with packed bed for long stick wood of length 68cm and thickness of 6cm, which is the basis of the development of our model [7,8].

Key components of this model include high gas velocity, a thin char reaction zone (<1 cm), and resolution of the steep temperature gradients in the bed. Thomas Reed and Markson [9] have modelled downdraft gasification of woody biomass up to 2.5 cm in diameter and 4 cm long, examining bed depth, particle size and moisture content. Kayal et al. [10] modelled the gasification of bundled jute sticks (15 cm long and 1 cm outer diameter) tied in to bundles with average diameter of 74 mm. These bundles are placed in a reaction cylinder such that the jute sticks are parallel to the airflow as might be expected. Of particular interest in this model is very thin oxidation and reduction zone (~10 cm) in comparison with the overall reaction chamber height (1.5 m). Dasappa and Paul [11] have analyzed the gasification for char particle size of 8 mm equivalent diameter. Although a limited number of numerical models of packed bed wood combustion and gasification are available, many numerical models of packed bed coal combustion and gasification have been reported. Bryden and Ragland [12] have analyzed the fixed bed combustor/gasifier for hardwood logs 20 cm in diameter, burned in a 3.7 m deep fuel bed. The state of the art for coal conversion was carefully reviewed by the Advanced Combustion Engineering Research Centre of the Brigham Young University (Provo, UT) Hopps et al. [13]. The common features adopted by the different models were identified and include:

1. single shape and size of the particle
2. no momentum transfer
3. constant porosity of the bed
4. heat and mass transfer coefficients for non reacting systems
5. instantaneous drying
6. instantaneous or highly simplified solid devolatilization
7. uncertainty on the intrinsic kinetics of heterogeneous combustion and gasification reactions
8. no homogeneous gas phase reactions apart from the water gas shift equilibrium
9. steady, one-dimensional equations
10. limited model sensitivity analysis and validation

It is also pointed out that "model development has not reached the point where significant use is made in process development for coal utilization," but some successive analyses presented by the same research group Ghani et al. [14]; Radulovic et al. [15] have contributed significantly to this issue through models that remove assumptions 3, 5, 6 and 10. The most recent study by Monazam and Shadle [16] aimed at the formulation of engineering calculations for updraft coal gasification is worth mentioning. Heterogeneous reaction kinetics and transport phenomena have been considered by Groeneveld and van Swaaij [17], Manurung and Beenackers [18] and Di Blasi [19]. All these analyses are for downdraft gasifier models reflecting the state of the art achieved in coal gasification.

In the present study, a model is presented that is comprehensive of the main physical and chemical processes of updraft packed bed gasification of long stick wood. Assumptions 1, 2, 3, 4, 7 and in part 9 (one-dimensional system; Hobbs et al. [13]) are still retained, but the model is dynamic, removes the other limitations, and takes into account the effects of axial heat convection, radiation and mass diffusion.

2. Experimental method

Fig. 1 shows the gasifier being modelled. Air is forced upward through the gasifier. Combustion takes place in the bottom portion of the gasifier, supplying heat for globally endothermic processes of gasification, pyrolysis and drying. In Kanchepuram District, of Tamil Nadu State, India Casuarina wood is harvested on a rotating basis with the plantations having short rotation period of 7–15 years. With plants spaced at 2 m apart, on a 7–10-year rotation, the wood yield is about 10–20 t ha^{-1} yr^{-1}. It dries in 5–10 days on the open sun drying. Also the bark is used for gasifier feed. The wood sample has been analyzed at the Madurai Kamaraj University, Department of Bio-Energy, in a Micro-TGA. The proximate and ultimate analysis of the Casuarina wood is presented in Table 1.

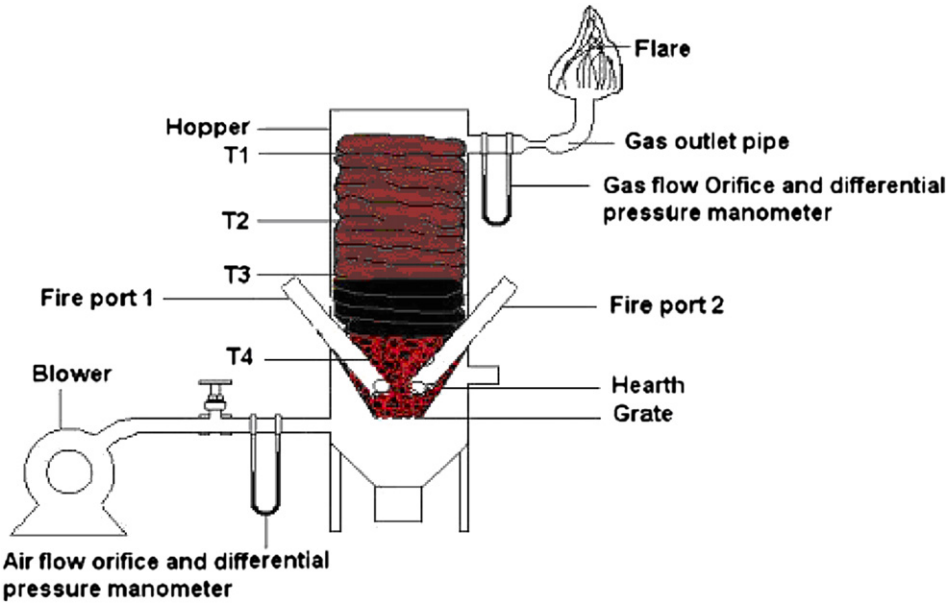

Fig. 1 – Pilot model for updraft long stick wood gasifier.

Temperatures in the actual gasifier were measured at fixed locations. Four separate thermocouple measurements were taken at a height of 0.25 m, 0.66 m, 0.78 m, and 0.92 m above the bottom of the gasifier using Type K thermocouples. The radiation temperature is around 100 °C. Thermocouple is shielded with ceramic tube. The outer sheath is made out of inconnel/ceramic tube with SS collar sleeve. The thermocouple head with dust proof die cast Aluminium head ceramic junction. The measurement of temperature ranges between 0 and 1200 °C. The temperature indicator is located separately far away minimum 1 m from gasifier. The thermocouple and indicator connected with temperature compensation cable.

During gasifier operation, the equivalence ratio for the gasifier is found to be in the range of 0.26–0.43. This is within the range for ideal and theoretical gasification (0.19–0.45). The air/fuel ratio increases from 1.25 to 8 as more and more of the charcoal are gasified and the process approaches complete combustion. The air/fuel ratio performance details are given in Table 2.

3. Model descriptions of the fixed bed gasifier

In the present work, there are several differences from the way in which gasifier beds have traditionally been modelled. Most gasifier models consider steady-state performance of a gasification system, with new wood materials added as char is consumed. In this gasifier operation, there is a fixed quantity of char that is combusted to gasify a fixed amount of wood, and the gasifier does not operate in a steady-state manner. This model is used to solve for the transient performance of a gasifier.

The numerical model describes the performance of the combustion and char surface reactions, drying and pyrolysis in the wood region, and the external gas phase reactions. The computational model describes the bed as a series of discretized solid particles that interact with each other and with the external gas volume. A schematic view of the discretization of the bed is shown in Fig. 2.

The lower portion of the bed consists of ten solid char particles and the gases that occupy the volume not filled by solid char particles. Each char particle is a single cell and is assumed to have a uniform temperature. The upper section of the bed is composed of ten wood particles as well as external gas volumes. The wood particles and external gas region are further discretized to compute temperature and pressure gradients within the wood particles, and to account for the steep concentration gradients within the gas region. The gas volumes are each 1 mm in size, the wood volumes are 0.333 mm in size, and each char volume consists of an entire char particle that is 4.8 cm in size.

Fig. 3 shows a close-up of an individual char particle. The char particles interact with each other through conductive and radiative heat transfer, and interact with the external gas layer through convective and radiative heat transfer. There are 48 gas volumes per 4.8 cm char particle.

Table 1 – Proximate and ultimate analysis of the Casuarina wood.

	Fixed carbon	Volatile matter	Moisture	Ash
Proximate analysis (in units of g kg^{-1} of wood)	174	656	150	20
	Carbon	Hydrogen	Oxygen	Nitrogen
Ultimate analysis (in units of g kg^{-1} of wood)	485	65	443.2	6.8

Table 2 – Performances of 5 h and 15 min run by the updraft gasifier.

Time, h	Flame temperature, °C	Airflow rate, $m^3 h^{-1}$	Gas flow rate, $m^3 h^{-1}$	Fuel flow, $kg h^{-1}$	Air/fuel	Mode
0:00	647	24	27	3.90	8	Combustion
0:15	676	25	28	3.90	8.33	Combustion
0:30	699	26	32	7.80	4.33	Combustion
0:45	715	27	34	9.10	3.86	Combustion
1:00	748	28	44	20.8	1.75	Pyrolysis
1:15	760	29	45	20.8	1.81	Pyrolysis
1:30	820	30	47	22.1	1.76	Pyrolysis
1:45	846	30	49	24.7	1.58	Pyrolysis
2:00	861	29	51	28.6	1.32	Pyrolysis
2:15	870	30	54	31.2	1.25	Pyrolysis
2:30	895	31	41	13.0	3.10	Pyrolysis
2:45	935	31	38	9.10	4.43	Pyrolysis
3:00	948	28	35	9.10	4.00	Pyrolysis
3:15	960	27	33	7.80	4.50	Char gasification
3:30	984	25	30	6.50	5.00	Char gasification
3:45	994	24	28	5.20	6.00	Char gasification
4:00	1000	23	27	5.20	5.75	Char gasification
4:15	1001	22	27	6.50	4.40	Char gasification
4:30	1000	21	27	7.80	3.50	Char gasification
4:45	995	20	27	9.10	2.86	Char gasification
5:00	900	20	27	9.10	2.86	Char gasification

In contrast to the char particles, the wood particles are not considered to be at a constant temperature (Fig. 4). Each wood particle is discretized into 180 finite volumes (only 10 shown in Fig. 4), with 60 external gas volumes per wood particle. This discretization of the wood particle is necessary to determine the performance of the wood particle under thermally thick or thermal wave conditions, where temperature gradients exist within the solid wood particle. The wood particle is modelled as a one-dimensional particle. Heat and mass transfer occur between the finite volumes within the solid wood particle. For the solution of the one-dimensional wood particle, only the surface of wood particle (the top and bottom finite volumes in Fig. 4) interacts with neighbouring wood particles or the surrounding gas layer. The temperature of the wood particle is assumed to vary linearly between T_{top} and T_{bottom} for determining the total amount of convective heat transfer between the wood particle and the surrounding gas volumes. In this manner, all of the 61 surrounding gas volumes will convert energy to/from the wood particle.

A detailed pyrolysis model Hagge [20] is used to describe the drying and pyrolysis of each of the ten wood particles. This model can predict pyrolysis products vs time for different sizes and shapes of particles under a wide range of pyrolysis conditions (thermally thin, thermally thick, and thermal wave pyrolysis regimes). By calculating the performance of individual particles, the computational model is able to determine

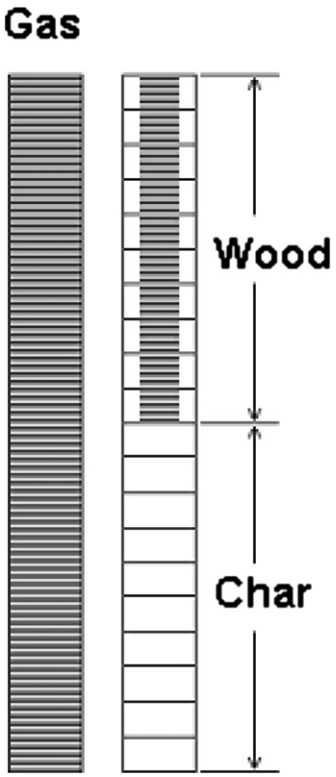

Fig. 2 – Gasifier bed.

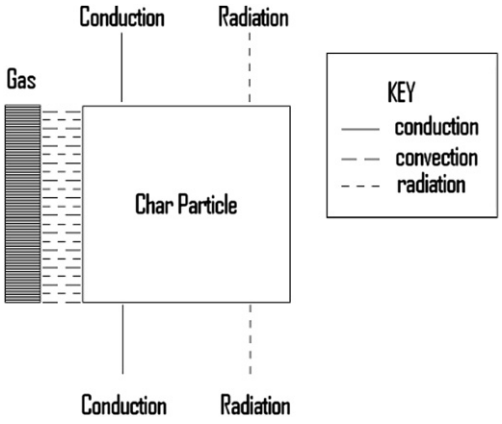

Fig. 3 – Interaction of a single char particle.

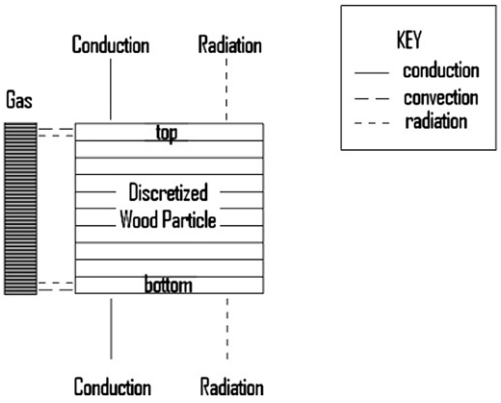

Fig. 4 – Interaction of a single wood particle.

the interaction between the combustion in the lower portion of the bed and the pyrolysis in the upper region. The model accounts for changes in operating conditions such as a change in the size of the char or wood particles, or the type of fuel being gasified. The ability to make changes based on the types of particles in a realistic manner gives this model an advantage over models that do not include individual particle performance. The computational domain is divided into an unstructured set of finite volumes. Basic conservation equations are enforced between each of the finite volumes and the resulting sets of equations are solved using Newton-GMRES procedures. These unstructured solution procedures are useful because they allow the same model to transition between one-dimensional and multi-dimensional particles, and allow interaction between any number of finite volumes, whether they are adjacent to each other or not (as in radiation). Although the discretization of the gasifier in this model can be thought of as one-dimensional (gas flow and heat transfer occur only in one direction), the solution procedures are not one-dimensional because each char particle interacts with two neighbouring char particles and 61 external gas volumes.

The basic conservation equations for a finite volume on an unstructured grid are computed as volume and surface integrals. In this manner, the same equations can be used for one-dimensional, two-dimensional, and three-dimensional conditions. Surface integrals are indicated explicitly while the volume integrals (such as the gas production term below) are implied but are not explicitly stated because properties are constant within each finite volume.

Conservation of total gas mass:

$$\frac{\partial m_G}{\partial t} + \oint \rho_G \vec{V} \cdot \hat{n} = \dot{\omega}_G \tag{1}$$

where m_G is the mass of gas within the finite volume, ρ_G is the density of the incoming/leaving gas volume, $\vec{V}$ is the velocity of the incoming/exiting gas, $\hat{n}$ is the direction normal to the surface of the particle, and $\dot{\omega}_G$ is the rate of production of gas.

The first term is the rate of storage of gas mass with respect to time. The second term represents the rate of mass that exits the finite volume, and the right hand term is the rate of gas production. Conservation of gas mass applies to the external gas phase finite volumes as well as void (gaseous) regions within the wood particle. Production terms for the external gas phase include gases produced/destroyed from the char surface reactions, from gas phase reactions, as well as gases released from the solid wood particles by drying and pyrolysis.

Conservation of momentum:

$$\vec{V} = -\frac{\phi}{\mu}\frac{\partial p}{\partial \hat{n}} \tag{2}$$

where $\vec{V}$ is the velocity of the exiting gas, ϕ is the permeability of the finite volume, μ is the kinematic viscosity, and $\partial p/\partial \hat{n}$ is the pressure gradient in the normal direction.

Darcy flow is assumed within the wood particle, and in the external gas volumes of the gasifier.

Conservation of gas species:

$$\frac{\partial m_I}{\partial t} + \oint \rho_I X_I \vec{V} \cdot \hat{n} = \dot{\omega}_I \tag{3}$$

where the subscript I indicates a particular gas species, and X_I is the mass fraction of species I.

Conservation of energy:

$$k\frac{\partial T}{\partial \hat{n}} + \oint h(T_\infty - T_i) + \oint \sigma\left(T_\infty^4 - T^4\right) - \oint \rho_G V c_G (T_n - T_i) + \sum \Delta h_I^\circ \dot{\omega}_I = \frac{\partial E}{\partial t} \tag{4}$$

where k is the thermal conductivity, h is the convective heat transfer coefficient, σ is the Steffan-Boltzman constant, c_G is the specific heat of the gas, T_i is the temperature at the finite volume under consideration, T_n is the temperature of a neighbouring finite volume, T_∞ is the external radiative temperature, Δh_I° is the enthalpy of formation of species I, and $\partial E/\partial t$ is the rate of energy storage with respect to time.

Energy can be transferred between finite volumes due to conduction, convection, radiation or mass transfer. Energy can be created or destroyed through exothermic/endothermic reactions. The net change in energy with respect to time is equal to the rate of energy storage.

4. Combustion, gasification and pyrolysis reactions

The basic reaction set is the same as in Bryden and Ragland [12]. The combustion reactions are modelled using the surface oxidation of char, as well as gas phase oxidation of CO to form CO_2. Any H_2 production is instantaneously converted into H_2O in the presence of oxygen. Additional char surface reactions include the reaction of char with H_2O and with CO_2.

where

$$h_{D_i} = D_i\left(2.0 + 1.1Re^{0.6}Sc^{1/3}\right)\phi/d, \quad \phi = 0.8 \quad \text{and} \quad T_e = 0.5(T_S + T_{Gas}) \tag{10}$$

$$k_1 = 13.4\exp(-32,600/(8.314 \times T_S)) \tag{11}$$

$$k_3 = 3.42T_S\exp(-1.56 \times 10^4/T_S) \tag{12}$$

$$k_4 = 1.67k_3 \tag{13}$$

Reaction scheme	($MJ\,kg^{-1}$)		
$2C + O_2 \rightarrow 2CO$	9.2	$\dot{\omega}_1 = \rho_{O_2} A_V (2M_C/M_{O_2}) h_{D_1} k_1/(h_{D_1} + k_1)$	(5)
$2CO + O_2 \rightarrow 2CO_2$	10.1		(6)
$C + CO_2 \rightarrow 2CO$	−14.4	$\dot{\omega}_3 = \rho_{CO_2} A_V (M_C/M_{CO_2}) h_{D_3} k_3/(h_{D_3} + k_3)$	(7)
$C + H_2O \rightarrow H_2 + CO$	−14.6	$\dot{\omega}_4 = \rho_{H_2O} A_V (M_C/M_{H_2O}) h_{D_4} k_4/(h_{D_4} + k_4)$	(8)
$2H_2 + O_2 \rightarrow 2H_2O$	142.9	Instantaneous	(9)

The competitive pyrolysis reaction scheme includes three primary pyrolysis reactions [21] to form tars, light gases, and char, and two secondary reactions of the tars within the particle to form light gases [22,23]. The competitive reaction scheme allows the products of pyrolysis to vary depending on the conditions under which pyrolysis occurs.

$$\text{wood} \xrightarrow{k_1} \text{tar}, \quad k_1 = 4.13 \times 10^6 \exp(-112,700/(8.314 \times T)) \tag{14}$$

$$\text{wood} \xrightarrow{k_2} \text{light gas}, \quad k_2 = 1.44 \times 10^4 \exp(-88,600/(8.314 \times T)) \tag{15}$$

$$\text{wood} \xrightarrow{k_3} \text{char}, \quad k_3 = 7.38 \times 10^5 \exp(-106,500/(8.314 \times T)) \tag{16}$$

$$\text{tar} \xrightarrow{k_4} \text{light gas}, \quad k_4 = 4.28 \times 10^6 \exp(-107,500/(8.314 \times T)) \tag{17}$$

$$\text{tar} \xrightarrow{k_5} \text{char}, \quad k_5 = 1.00 \times 10^5 \exp(-107,500/(8.314 \times T)) \tag{18}$$

5. Gasifier conditions

The gasifier is heated through two fire ports located near the center of the charcoal region at temperatures of around 500 °C. The fan is operated in suction mode which results in preferential heating at the bottom portion of the char bed. The heat-up phase lasts approximately ten minutes, when the gasifier bed has reached sufficient temperatures to sustain combustion. The fan direction is switched and gases are pushed upward through the gasifier at a controlled rate. The gasifier contains 10 kg of charcoal in the lower portion of the bed and 60 kg of wood in the upper portion of the bed.

Numerically, this heat-up phase is handled somewhat crudely, as the existing model is not currently being used to study ignition. In the numerical model, the gasifier initially contains 98% N_2 and 2% O_2. A constant velocity of air (21% O_2 79% N_2) is blown upward through the gasifier under both the ignition and normal operation. The ten char particles each receive a source heating term of 50 W in addition to any gains or losses from the conservation reactions. When all of the char particles reach a temperature of at least 450 °C, the heating source term is stopped and the char particles heat-up according to the equation sets.

The lower portion of the bed contains 10 kg of dry char particles, is 48 cm tall, and contains a total horizontal cross-sectional area of 0.36 m^2. The numerical model contains only 10 cylindrical char particles with an initial length of 0.09 m, a diameter of 0.048 m, and a density of 100 $kg\,m^{-3}$. The performance of each individual char particle in the numerical model is multiplied by 61.40 to obtain a total mass of 10 kg of char, and used to determine the total amount of interaction with the external gas phase. As devolatilization of the char particle occurs, the diameter and the length are reduced proportionally ($d/d_o = l/l_o$). The amount of radiation between char particles is based on two particles with a 1 mm gap between them. The view factor between the particles is calculated using two coaxial parallel disks [24] that are spaced ($1\,mm + r_i + r_j$) apart with diameters that vary according to the degree of combustion of the char particle.

$$R_i = r_i/L, \quad R_j = r_j/L, \quad S = 1 + \frac{1 + R_j^2}{R_i^2} \tag{19}$$

$$F_{ij} = \frac{1}{2}\left\{S - \left[S^2 - 4\left(r_j/r_{ii}\right)^2\right]^{1/2}\right\} \tag{20}$$

The bottom-most char particle radiates to a specified temperature, in K, with a constant view factor of 0.5, while the top-most char particle radiates to the temperature of the bottom-most wood particle, with a view factor according to their diameters. The temperature that the bottom char particle radiates to is as follows:

$$T_{rad} = 300, \quad T_S < 400 \tag{21}$$

$$T_{rad} = (T_S - 100), \quad 400 < T_S < 1100 \tag{22}$$

$$T_{rad} = 1000, \quad T_S > 1100 \tag{23}$$

The total amount of radiation heat flux between particles depends on their view factors, their respective areas, and their temperatures.

$$\dot{Q}_{ij} = A_{V_i} \cdot F_{ij} \cdot 0.9\sigma\left(T_i^4 - T_j^4\right) \tag{24}$$

The upper portion of the bed contains 60 kg of wet (15% moisture content, wet basis) wood, is 60 cm tall and contains a

horizontal cross-section of 0.36 m^2. The numerical code models 10 cylindrical wood particles with a diameter of 6 cm and a length of 68.58 cm, and a dry density of 600 kg m^{-3}. The performance of the ten wood particles are each multiplied by 4.38 to obtain a total mass of 60 kg, and to determine the correct interaction with the external gases in the upper portion of the bed.

The external gas phase has conduction between adjacent gas volumes, convection to the solid particles, and radiation between the gas and the solid particles. The thermal conductivity of the gas is given by

$$k_{gas} = 2.495 \times 10^{-3} \frac{T_{gas}^{1.5}}{T_{gas} + 194} \ \mathrm{W\,m^{-1}\,K} \quad (25)$$

At the top and bottom of the gasifier, there is a temperature gradient of 5 K m^{-1}.

Radiation occurs between the solid particle and the 60 gas volumes.

$$\dot{Q}_{rad,solid\rightarrow gas} = F_{gas} \times 0.9 \frac{A_V}{60}\sigma\left(T_S^4 - T_{gas}^4\right)56.59 \quad \text{where } F_{gas} = 0.02 \quad (26)$$

Convection occurs between the solid particle and the 60 gas volumes at the film temperature, defined as the average of the surface and external gas temperature, and is as follows:

$$\dot{Q}_{conv,solid\rightarrow gas} = h \frac{A_V}{60}\left(T_S - \frac{T_S + T_{gas}}{2}\right)61.40 \quad (27)$$

where

$$Nu = 1.1 Pr^{1/3} Re^{0.6}, \quad h = Nu \times k_S/d \quad (28)$$

As the size of the char particle is reduced, the amount of convection and radiation from the solid particle to the gas phase is reduced. The computational model stops including the effects of the char particle when their diameters are less than 1 μm.

The detailed pyrolysis of each of the ten wood particles is calculated. This includes conservation of mass, momentum and energy within the particle, changes in physical properties (conductivity, density, specific heat, permeability, etc.) at different locations within the particle as the particle is converted from wood to char, and competitive pyrolysis reactions. The numerical code computes the drying, the pressure gradient, the release of primary pyrolysis gases within the particle, and the conversion of these primary pyrolysis products to secondary products as they move through the solid particle. This code combines the detailed pyrolysis of ten particles, and the interaction between each of the particles, and the external gas layer.

The combustion and gasification regions are also coupled. Gasification depends on the products being released in the combustion region, as well as the pyrolysis of the wood region. The combustion of the charcoal region is dependent on the amount of heat transfer to the cooler wood bed above. The gasifier is a tightly coupled system in which combustion and gasification are modelled in conjunction with a detailed pyrolysis model. This type of model has unique capability to compute changes in gasifier performance based on changes in operating conditions that simplified models would not be able to handle. The drawback is that the code can only compute 500 s of gasifier performance per hour on a Pentium M 1.6 due to the complexity of the calculations.

6. Performance of individual wood and char particle within the gasifier

Each wood particle is divided into 180 cells in the computational model. The total dry mass of the wood particle is 1.16 kg, with each cell having an initial wood mass of 6.46 g. Each of these wood cells has an initial water mass of 1.13 g (1.13 = 15% of 7.59). The performance of the individual particles is calculated in the computational model. The temperatures of the ten wood particles after 1, 2, 3 and 4 h of operation are shown in Fig 5.

Each dip represents the temperature at the center of each of the 10 particles, with the peaks at the surface of each particle. Throughout the gasification process, there is a 200 to 300 K temperature difference within different regions of the wood particles.

Fig. 6 shows where/when wood is being pyrolyzed during the gasification process.

The first 2 h of char combustion dry and heat the wood particles. The wood profile shows that only the outer surfaces of the bottom-most wood particles have been pyrolyzed after 2 h of operation. At 3 h, pyrolyzation is occurring through the entire wood particles. The centers of the particles have a much higher wood concentration because of the time needed to heat-up and dry the interior of the pieces of wood. By matching the regions where 50% of the wood has been pyrolyzed (Fig. 6) with the temperatures at the same location (Fig. 5), the temperature profiles at $t = 3$ h show that pyrolyzation occurs with wood temperatures between 700 and 850 K for this gasifier. At 4 h of operation the bottom-most wood particles have been completely pyrolyzed and only the top 5 wood particles have significant amounts of wood remaining.

During devolatilization, the total mass of the particle is composed of both wood and char. Fig. 7 shows the char mass within each of the ten particles.

Each wood cell started with 6.46 g of wood, and ends up with around 2 g of char after pyrolysis is complete, with the rest released as volatiles. The mass of the char is about 30% of the original mass of the wood (dried mass). The char density

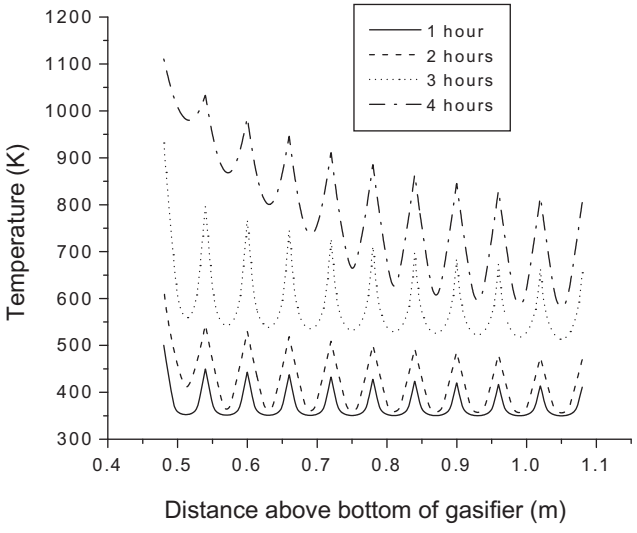

Fig. 5 – Wood particle temperatures.

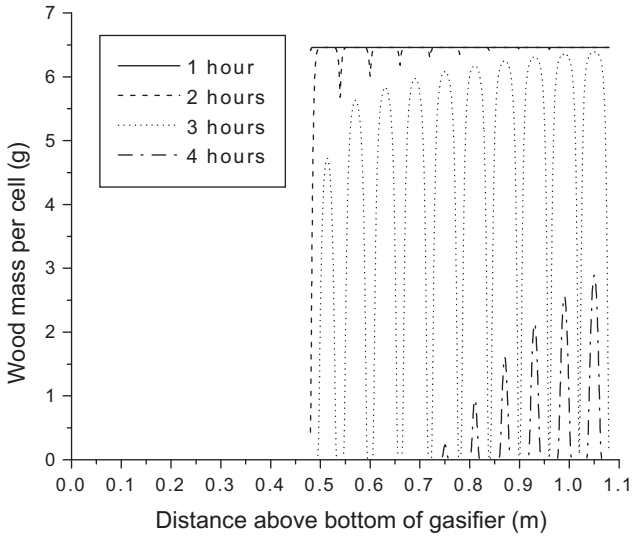

Fig. 6 – Wood profile at selected times.

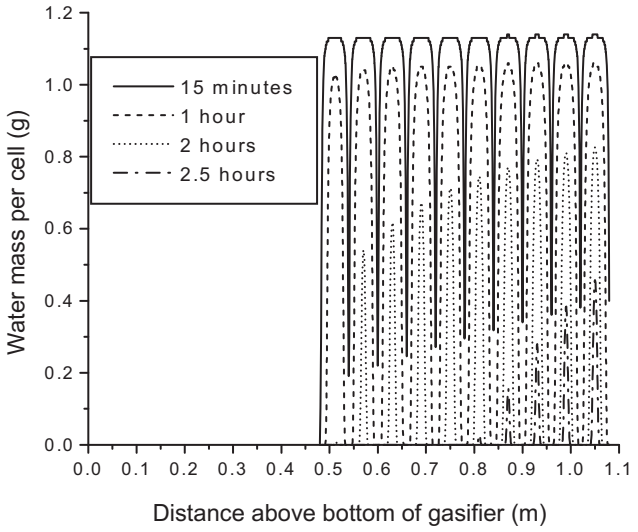

Fig. 8 – Moisture profile at selected times.

varies slightly within the particles (see $t = 4$ h) when devolatilization is complete, because pyrolysis temperatures differ at the outer and inner regions of the particle (higher pyrolysis temperatures produce more volatiles and less char).

Fig. 8 shows the moisture profile within the ten wood particles.

The surfaces of the wood particles are dried first, while water remains at the interior of the particles. Only a small amount of drying occurs during the first hour of operation. The bottom-most wood particle is dried completely by $t = 2$ h, the bottom six wood particles are dried by $t = 2.5$ h, and the top four wood particles are dried completely shortly after $t = 2.5$ h. As temperatures at the surface of the particle increase, pressure builds near the surface and water is initially driven both out of the particle and towards the center of the particle. Soon after, the pressure in the interior builds sufficiently to drive moisture out of the entire particle (not shown). The bottom-most wood particle in the gasifier is completely dried within the first two hours, while it takes up to three hours for the top-most wood particle to dry. The combined temperature, wood, char, and moisture profiles show that while drying and pyrolysis happen mostly sequentially in each particle, the gasifier is not physically divided into separate drying and pyrolysis regions.

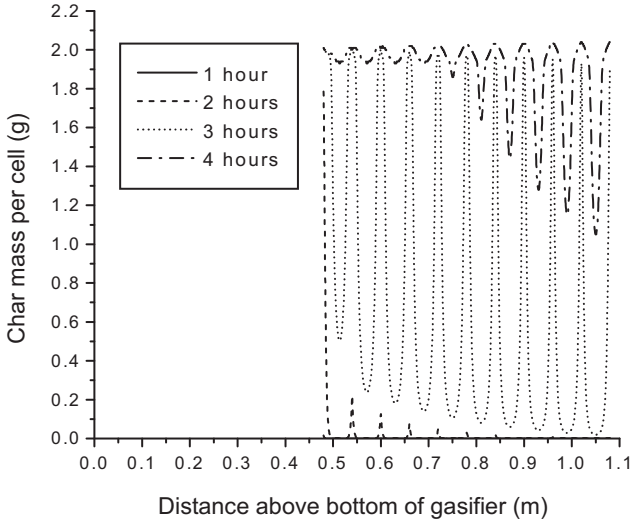

Fig. 7 – Char profile at selected times.

7. Results and discussions

7.1. *Comparison of experiment with the computational gas temperatures within the gasifier*

The results from the numerical code for an incoming airflow rate of 20 $m^3 h^{-1}$with moisture content of 15% on a wet basis are shown below. A comparison of the computational model with the experimental gas temperatures is shown in Table 3.

Temperatures in the actual gasifier were measured at fixed locations. The particles in the computational model move with respect to these fixed locations. For comparison, the height of the particles in the computational model is solved over time, and the temperature readings for a given height are compared to the experimental data. The thermocouple measurements were taken at a height of 0.25 m, 0.66 m, 0.78 m, and 0.92 m above the bottom of the gasifier. The experimental and numerical temperatures are shown in Fig. 9.

The four locations in Fig. 9 have previously been described as combustion, reduction, pyrolysis, and drying locations, respectively. Large particles of wood (>1 cm) may contain char at the surface of the particle and wet wood in the interior of the particle. This would indicate that four distinct regions do not exist during much of the combustion/gasification process. The open symbols in Fig. 9 show the predicted gas temperatures at the same locations as the thermocouples. Overall, the computational model appears to do a good job of describing the gasification process. Both the computational model and the thermocouple readings indicate that the gasifier heats up the wood particles for the first 2.5 h of operation, and that significant gasification occurs only in the second half of

Table 3 – Comparison of the computational model with the experimental gas temperatures.

Computational					Experimental				
Time (min)	$x = 0.25$ m	$x = 0.66$ m	$x = 0.78$ m	$x = 0.92$ m	Time (min)	$x = 0.25$ m	$x = 0.66$ m	$x = 0.78$ m	$x = 0.92$ m
	Combustion	Reduction	Pyrolysis	Drying		Combustion	Reduction	Pyrolysis	Drying
5	532	464	455	345	5	529	448	428	341
10	633	578	560	341	10	658	581	548	355
15	762	553	536	521	15	766	536	494	440
30	860	571	552	534	30	811	531	499	452
45	916	593	571	551	45	835	531	498	453
60	961	608	584	563	60	867	549	497	464
75	1005	622	597	574	75	892	570	494	499
90	1005	622	597	574	90	898	561	521	501
105	1063	647	617	591	105	984	516	522	513
120	1132	678	644	615	120	1011	517	521	532
135	1150	718	682	651	135	1059	519	523	538
150	1155	751	718	689	150	1107	526	538	545
165	1190	806	770	741	165	1128	561	546	547
180	1114	932	894	861	180	1169	570	561	558
195	1230	848	828	809	195	1189	582	578	575
210	1240	806	791	776	210	1204	600	592	587
225	1251	800	786	771	225	1215	618	609	592
240	1220	779	768	756	240	1227	762	647	601
255	1230	708	704	698	255	1241	786	682	609
270	1245	537	541	544	270	1259	529	520	450
285	1268	356	359	362	285	1278	329	331	350
300	1266	326	326	332	300	1277	361	347	362

gasifier operation (as evidenced by the increase in gas temperatures at $x = 0.66$, 0.78 and 0.92 m at 2.5 h). The major difference seems to be that the numerical model predicts lower combustion temperatures of 1120 to 1260 K, while actual thermocouple readings are as high as 1300 K. Also, the temperatures in the numerical model are closer to each other than in the actual gasifier.

There could be many reasons for differences between the numerical and experimental model. Likely candidates include the limitations of describing a three-dimensional system with a one-dimensional particle model, the breaking apart and movement of particles to replace empty space at the bottom of the pile, and inaccuracies in the predicted height of the pile in the computational model. In reality, there will be a larger number of small char particles at the bottom of the char pile than the numerical model predicts, which would both produce higher peak combustion temperatures and a lower mean distance for radiant heat transfer upward through the bed (smaller particle fill the bed more completely and block radiation upward through the bed). The experimental data also seems to indicate that the gasifier will burn for a slightly longer period of time, but this is likely due to the combustion of some of the newly charred particles (originally wood particles) at the end of the run. This combustion is not allowed in the computational model.

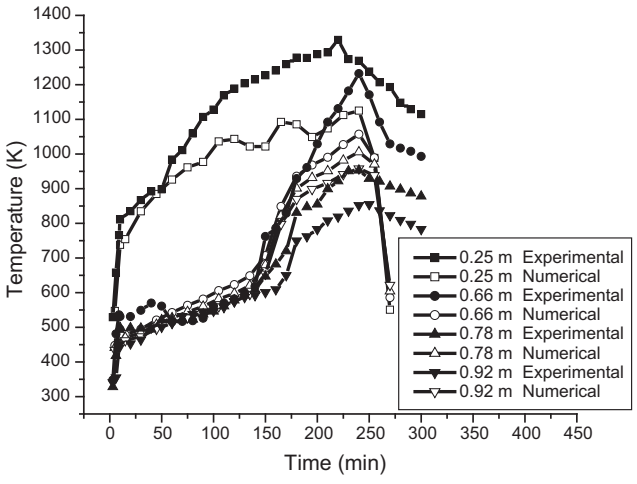

Fig. 9 – Experimental versus numerical gasifier temperatures.

7.2. *Gas profiles at different hours in the gasifier*

The gas profiles at $t = 1$ h is shown in Fig. 10.

At the gasifier entrance, oxygen and nitrogen enters into the gasifier at 300 K. Char combustion reactions consume the oxygen in the first 0.1 meters of the gasifier, and CO is produced. The mass fraction of nitrogen drops because additional gases are being produced from the combustion reaction. This combustion gas (CO and N_2) travels through the gasifier. At $x = 0.48$ m, the gases enter into the wood region, where water vapour is being released from drying wood particles. The mass fraction of N_2 and CO drop from $x = 0.48$ m to the gasifier exit at $x = 1.08$ m due to the additional mass of water vapour.

The gas profiles are similar at $t = 2$ h as shown in Fig. 11.

The x-location represents the original location within the bed. Oxygen is now consumed from $x = 0.038$ m to $x = 0.200$ m, indicating that the first 0.038 m of char have been consumed. A small amount of tars and light pyrolysis gases are released in the top portion of the gasifier.

The gas profile at $t = 3$ h is shown in Fig. 12.

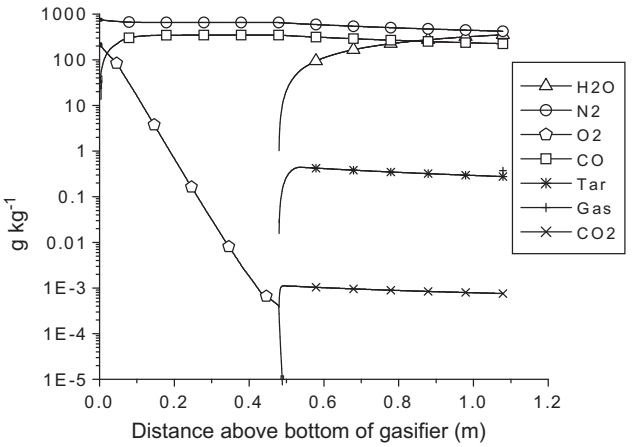

Fig. 10 – Gas profiles at t = 1 h in the gasifier.

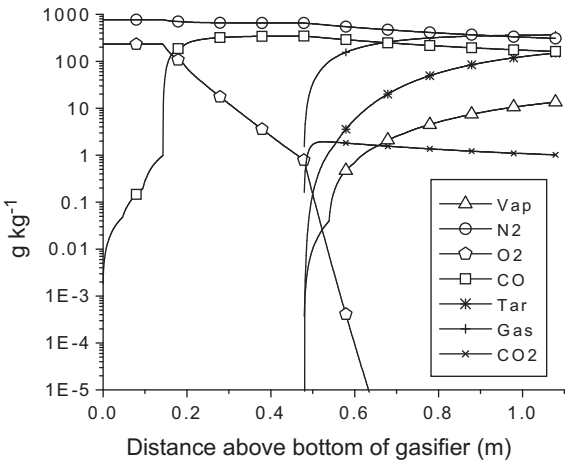

Fig. 12 – Gas profiles at t = 3 h in the gasifier.

At $t = 3$ h, the char combustions has moved to higher and higher char particles. Very little water is being released because most of the wood particles are completely dried. A large amount of light pyrolysis gases and a lesser amount of tars are released from the pyrolysis reactions. The 6 cm wood particles are large enough that tars produced within the active pyrolysis zone of the particle can be broken down within the wood particle into lighter pyrolysis gases (CO, H_2O, CO_2, CH_4, H_2) These light pyrolysis gases are not specifically modelled at this time, although it is common to assume a pyrolysis composition based on experimental data.

Until now, the char combustion is within a specific region (approx 0.15 m tall), and only a negligible amount of oxygen reaches the wood portion of the bed. The model assumes that CO, O_2, and H_2O are all necessary for a three body collision that converts CO to CO_2. The model assumes no H_2O in the char region. The lack of H_2O in the char region, and the lack of O_2 in the wood region results in no CO_2 production from the char combustion reactions. CO_2 concentration would increase dramatically if moisture were present in the oxygen regions of the gasifier. CO_2 may be present from the pyrolysis reactions, as part of the light pyrolysis gases.

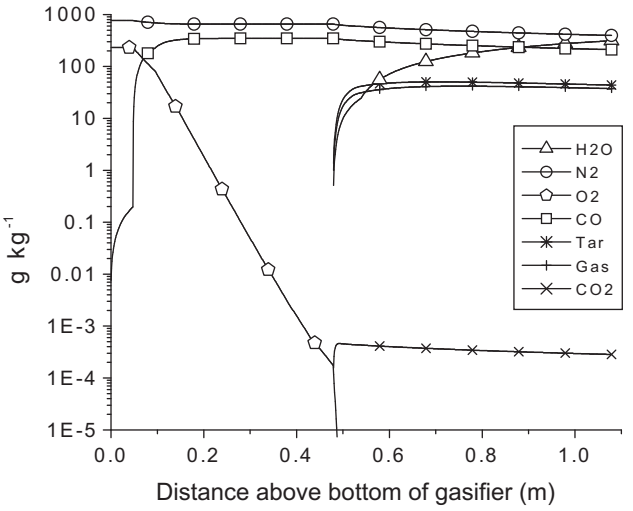

Fig. 11 – Gas profiles at t = 2 h in the gasifier.

The gas profile at $t = 4$ h is shown in Fig. 13.

Near the end of the gasifier operation, a small amount of O_2 survives into the wood region (which is now mostly char). A small amount of CO is converted into CO_2 at this time. The newly formed char from the wood is not allowed to combust in the model. Only light pyrolysis gases are produced (very little tar) at this time, because the pyrolysis gases are coming from pyrolyization of the center of the wood particles. The tars produced at the center of the particle are converted into light pyrolysis gases before they can escape the wood particle.

7.3. *Effects of external gas temperatures within the gasifier*

Fig. 14 shows the external gas temperature predicted by the numerical model for the charcoal portion of the bed.

The numerical model predicts that it takes about 2 h for the gasifier to get up to operating temperature, with an external gas temperatures of around 1260 K at $t = 2$ h. Nine peaks can be seen in the external gas temperature profile, where each peak corresponding to the combustion of one of the ten char particles. These combustion temperature ranges from 1260 K to 1120 K within the lower portion of the gasifier.

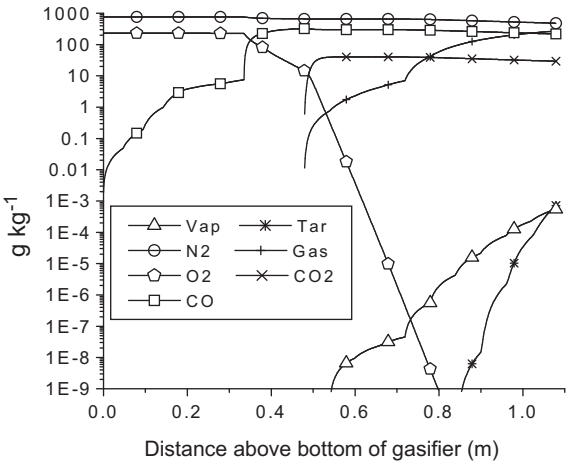

Fig. 13 – Gas profiles at t = 4 h in the gasifier.

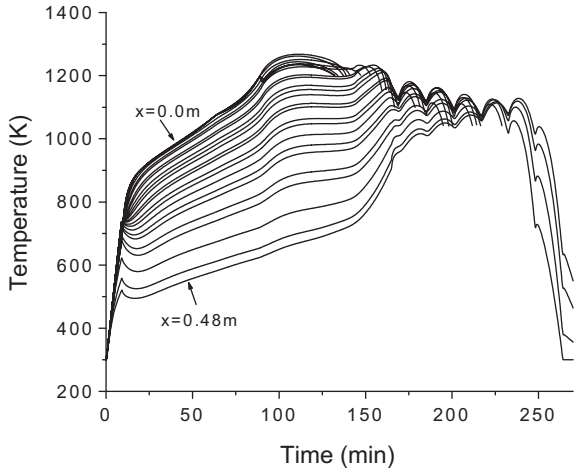

Fig. 14 – Char region gas profiles.

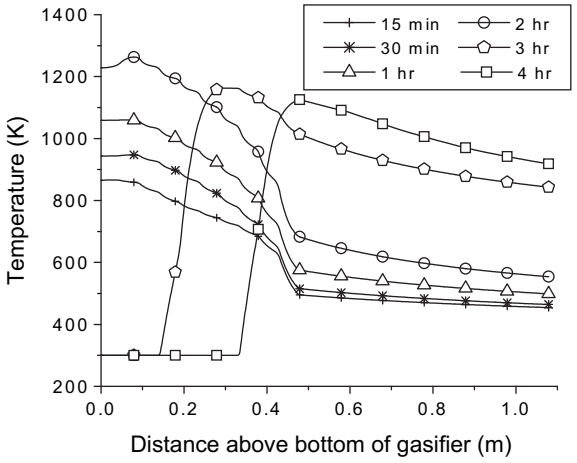

Fig. 16 – External gas temperature profile.

7.4. *Effect of devolatilization of the individual wood particles*

The devolatilization of the individual wood particles is shown in Fig. 15.

As expected, external gas temperature has to reach around 800 K (at t = 2.5 h) before significant amounts of pyrolysis can occur. The numerical model predicts that all ten wood particles will be gasified, and that nine of the ten char particles will be completely combusted. The numerical model does not allow for combustion of the wood particles. When the numerical model has one char particle left, there is not sufficient energy to maintain combustion.

7.5. *Effects of temperature profile of the gases at selected times*

Fig. 16 shows the temperature profile of the gases at selected times.

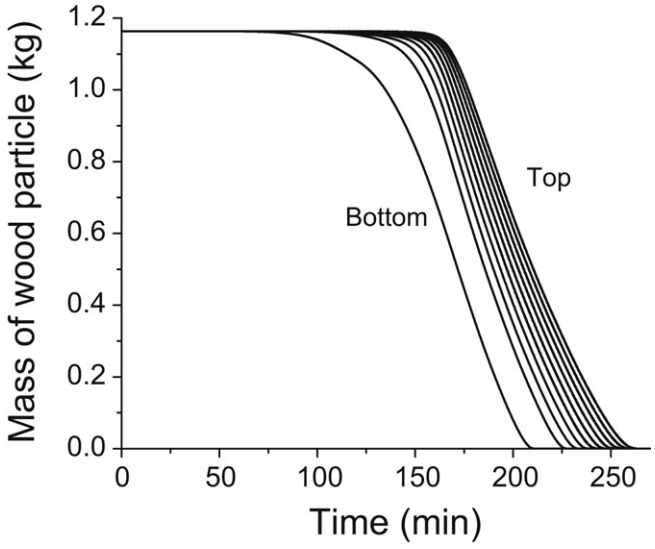

Fig. 15 – Devolatilization of 10 wood particles.

The numerical model predicts that it takes 2 h to get the gasifier full operating temperature (1260 K). The gas temperatures cool to 1120 K near the end of the run. Empty gas cells replace the original char particles and the model uses these gas cells to compute the temperature profile of what would be gases below the bottom-most char particles. The correlation between the numerical model and the experimental data could be improved by directly computing the entrance region throughout the run (rather than through boundary conditions) and by including the change in gasifier area in the char region.

7.6. *Comparison of the external gas temperatures for gasifier runs with two different moisture contents*

The computational model can be used to determine how a change in the moisture content of the wood affects gasifier performance. A second run was completed with 51 kg of dry wood and 18 kg of water, as opposed to 51 kg of wood and 9 kg of water in the previous run. All other conditions were identical to the previous run. Fig. 17 compares the external gas

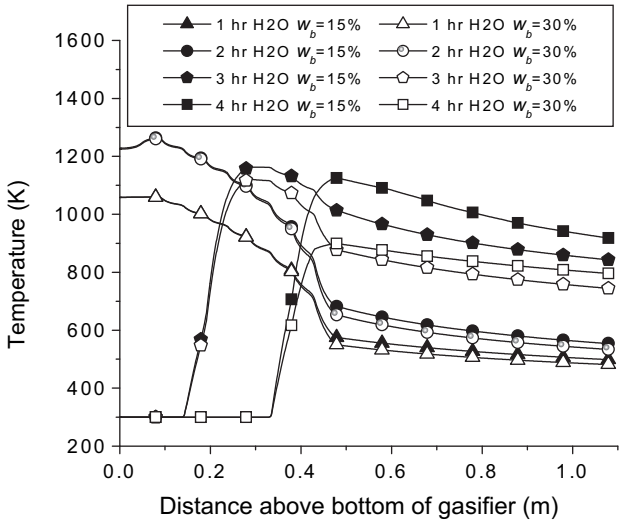

Fig. 17 – Numerical moisture predictions.

temperatures for gasifier runs with two different moisture contents (15% moisture versus 30% moisture on a dry basis).

In the first 2 h of gasifier operation, the performance during the initial heat-up period of the gasifier does not change much with the moisture content of the wood. In the wet wood (with twice as much water), the gas temperatures are 20–30 K cooler within the wood portion of the gasifier, while combustion temperatures are initially identical. After 3 h of operation, the wet wood begins to decrease the temperatures in the combustion region. After 4 h of operation there is a large difference (200 K) in the gas temperatures in the wood region.

8. Conclusions

A computational model for a fixed bed bottom lit updraft gasifier utilizing thermally thick long stick wood biomass fuel has been developed and evaluated with field test results. The gasifier obtained high-energy release rates due to the lower inlet air velocity and extended reaction zone. The model has been used to investigate the operating characteristics of the gasifier. The lowest portion of the bed is an oxidizing region and the remainder of the bed acts as gasification and drying zone for the 10 kW design case with 15% fuel moisture using under fire with an inlet velocity of $1\ m\ s^{-1}$. The operating characteristics of this type of gasifier provide a range of options for bed height as well as under fire airflow rate to obtain a desired heat release rate. This flexibility in operating condition is a significant aid in the design and start-up of the unique type of biomass power source.

The model includes the interactions between detailed wood particle performance, char particles, and the external gas phase. Because the model considers basic particle–particle interactions, the model can be applied to many different systems and is not limited to a narrow range of experimentally validated conditions. The model predicts the products of pyrolysis, the amount of char produced during pyrolysis occurs, as well as the residence times of the pyrolysis gases within the particle. This model also accounts for the interaction between the various regions of the gasifier in which char combustion, external gas, wood drying and/or pyrolysis may occur. The model predicts significant temperature (~200 K) changes within individual particles, and contradicts the idea that there are continuous and separate regions of drying and pyrolysis (at least in this size of particle). With the improved representation of the computational model, changes in wood diameter, char diameter, total height of the bed, wood moisture content and many other changes can be accounted for. The particle accuracy can be increased with improved particle models (two or three-dimensional particles) without changing the solution procedures.

The hope of the particle model is to produce models that are valid under a much broader range of conditions and that do not require "fitted" parameters. This type of model would lead future researchers to seek more detailed information about particle interactions within a packed bed, and in doing so learn more about gasification systems.

What can be learned from the computational model? In the current operation of the actual gasifier, the airflow rate is increased to maintain a certain incoming air to fuel ratio. The computational model indicates that all incoming air is consumed in the charcoal combustion region, and that maintaining a specific air/fuel ratio may be a poor measure of gasifier performance, because there are complicated interactions between various regions of the gasifier. Increasing the incoming airflow will increase combustion temperatures, which eventually will increase the rate of gasification, but not in a clear manner. Higher combustion temperatures gasify in less time, but may waste more energy due to energy carried out by the hot exhaust gases. The ideal operation of the gasifier can be determined by understanding all the important interactions in the gasifier from the computational model. Air to fuel ratio would be a more useful measure when moisture is present in the lower portion of the bed to maximize/minimize specific gasification products.

Acknowledgments

One of the authors Dr. A. Saravanakumar thank the Ministry of New and Renewable Energy, Government of India, for financial support in the form of fellowship under the National Renewable Energy Fellowship Programme from the year of 2000 to 2006.

Nomenclature

m_G	Mass of gas within the finite volume
ρ_G	Density of the incoming/leaving gas volume
$\vec{V}$	Velocity of the incoming/exiting gas
$\hat{n}$	Direction normal to the surface of the particle
$\dot{\omega}_G$	Rate of production of gas
ϕ	Permeability of the finite volume
μ	Kinematic viscosity
$\frac{\partial p}{\partial \hat{n}}$	Pressure gradient in the normal direction
k	Thermal conductivity
h	Convective heat transfer coefficient
σ	Steffan-Boltzman constant
c_G	Specific heat of the gas
T_i	Temperature at the finite volume under consideration
T_n	Temperature of a neighbouring finite volume
T_∞	External radiative temperature
Δh_i^o	Enthalpy of formation of species i
$\frac{\partial E}{\partial t}$	Rate of energy storage with respect to time
A_V	Surface area per unit volume
d	Diameter
M	Molecular Weight
h_D	Mass transfer coefficient
k	Reaction rate constant
T_s	Solid temperature
T_{Gas}	Gas temperature
$\dot{\omega}$	Reaction rate per unit volume
T	Absolute temperature
$R_{i,j}$	Yield of species i in reaction j on a mass species
F_{ij}	View factor
$\dot{Q}$	Total amount of radiation heat flux

k_{gas} Thermal conductivity of gas
$\dot{Q}_{rad,solid\rightarrow gas}$ Radiation between solid particle and gas volumes
$\dot{Q}_{conv,solid\rightarrow gas}$ Convection between solid particle and gas volumes
Nu Nusselt number
Pr Prandl number
Re Reynolds number

REFERENCES

[1] Di Blasi C. Processes of flames spreading over the surface of charring fuels: effects of the solid thickness. Combust Flame 1994;97(2):225–39.
[2] Di Blasi C. Predictions of wind-opposed flame spread rates and energy feedback analysis for charring solids in a microgravity environment. Combust Flame 1995;100(1, 2):332–40.
[3] Antal MJ, Varhegyi G. Cellulose pyrolysis kinetics: the current state of knowledge. Ind Eng Chem Res 1995;34(3):703–17.
[4] Brewster BS, Hill SC, Radulovic PT, Smoot LD. Fundamentals of coal combustion: for clean and efficient use. Chapter 8. In: Smoot LD, editor. Comprehensive modeling. Netherlands: Elsevier Science Publishers; 1993. p. 567–712.
[5] Albini FA, Reinhardt ED. Modelling ignition and burning rate of large woody natural fuels. Int J Wild Land Fire 1995;5(2):81–91.
[6] Purnomo D, Aerts J, Ragland K. Pressurized downdraft combustion of wood chips. P Combust Inst 1990;23(1):1025–32.
[7] Saravanakumar A, Haridasan TM, Reed TB, Kasturi Bai R. Operation and modelling of an updraft long stick wood gasifier. Energ Sustain Dev 2005;9(4):25–39.
[8] Saravanakumar A, Haridasan TM, Reed TB, Kasturi Bai R. Experimental investigations of long stick wood gasification in a bottom lit updraft fixed bed gasifier. Fuel Process Technol 2007;88(6):617–22.
[9] Reed TB, Markson M. A predictive model for stratified downdraft gasification of biomass. Proceedings of the Fifteenth Biomass Thermochemical Conversion Contractors Meeting, Atlanta, GA; 1983. 38 pp.
[10] Kayal TK, Chakravarty M, Biswas GK. Mathematical modelling of continuous updraft gasification of bundled jute stick – a low ash content woody biomass. Bioresource Technol 1994;49(1):61–73.
[11] Dasappa S, Paul PJ. Gasification of char particles in packed beds: analysis and results. Int J Energy Res 2001;25(12): 1053–72.
[12] Bryden KM, Ragland KW. Numerical modelling of a deep, fixed bed combustor. Energy Fuel 1996;10(2):269–75.
[13] Hopps ML, Radulovic PT, Smoot LD. Combustion and gasification of coal in fixed beds. Prog Energ Combust 1993; 19(6):505–86.
[14] Ghani MU, Radulovic PT, Smoot LD. An improved model for fixed bed coal combustion and gasification: sensitivity analysis and applications. Fuel 1996;75(10):1213–26.
[15] Radulovic PT, Ghani MU, Smoot LD. An improved model for fixed bed coal combustion and gasification. Fuel 1995;74(4): 582–94.
[16] Monazam ER, Shadle LJ. Predictive tool to aid design and operation of pressurized fixed bed coal gasifiers. Ind Eng Chem Res 1998;37(1):120–30.
[17] Groeneveld MJ, Van Swaaij WPM. Gasification of char particles with CO_2 and H_2O. Chem Eng Sci 1980;35(1, 2): 307–15.
[18] Manurung RK, Beenackers AACM. Modelling and simulation of an open core downdraft moving bed rice husk gasifier. In: Bridgwater AV, editor. Advances in thermochemical biomass conversion. London: Blackie Academic & Professional; 1992. p. 288–309.
[19] Di Blasi C. Dynamic behaviour of stratified downdraft gasifiers. Chem Eng Sci 2000;55(15):2931–44.
[20] Hagge MJ. A numerical model for biomass pyrolysis. Ph.D. thesis, Department of Mechanical Engineering, Iowa State University, USA; 2005.
[21] Thurner F, Mann U. Kinetic investigations of wood pyrolysis. Ind Eng Chem Proc DD 1981;20(3):482–8.
[22] Liden AG, Berruti F, Scott DS. A kinetic model for the production of liquids from the flash pyrolysis of biomass. Chem Eng Commun 1988;65(1):207–21.
[23] Di Blasi C. Analysis of convection and secondary reaction effects within porous solid fuels undergoing pyrolysis. Combust Sci Technol 1993;90(5, 6):315–40.
[24] Howell JR. A catalogue of radiation configuration factors. New York: McGraw-Hill; 1981.